

Comparison of Conductometric Gas Sensitivity of Surface Acoustic Wave Modes in Layered Structures

David A. Powell,^{1,*} Kourosh Kalantar-zadeh,² Samuel Ippolito,² and Wojtek Wlodarski²

¹*School of Electrical and Computer Engineering, RMIT University, Melbourne, Australia*

²*CRC for Microtechnology, Melbourne, Australia*

(Received: 6 May 2004. Accepted: 20 January 2005.)

Properties of propagation modes for a layered ZnO/XZ LiNbO₃ surface acoustic wave sensor have been investigated both theoretically and experimentally. By calculating the effective permittivity function, it was shown that after the ZnO deposition two distinct propagation modes have been generated: a Rayleigh and a shear horizontal. A layer of InO_x was deposited to provide a conductometric sensing mechanism to NO₂. It was found that the sensor is at least one order of magnitude more sensitive when operating in Rayleigh mode than in the shear horizontal mode. This sensitivity was found to be in good agreement with calculations for low concentrations of NO₂, however discrepancies were observed for higher concentrations.

Keywords: SAW Gas Sensor, Layered, Conductometric, ZnO, InO_x, NO₂.

1. INTRODUCTION

Surface Acoustic Wave (SAW) devices are effective tools for gas sensing applications at ppm and ppb levels. The first application of a SAW device for gas sensing was reported by Wohltjen and Dessy¹ in 1979. In this work, the velocity change of an acoustic wave was found to be proportional to the mass adsorbed onto the active surface of the device. This velocity change is easily measured as a frequency change when the SAW device is used as the resonant element in an oscillator. Another principal by which SAW sensors can operate is a change in conductivity on the active surface,² as the acoustic wave properties of piezoelectric materials are highly sensitive to electrical boundary conditions. SAW structures have been developed for sensing numerous gases and vapours including H₂,^{3,4} SO₂,⁵ NO_x,⁶ and NH₃,⁷ amongst many others.⁸

Although a configuration of a piezoelectric guiding layer on a piezoelectric substrate has been employed for RF filters and resonators, such structures are still not widely used for gas sensing applications, despite the advantages which they offer. The authors previously demonstrated

that a piezoelectric layer deposited onto the piezoelectric substrate can increase the conductometric sensitivity of a SAW device.⁹ Such a layer also protects the metal inter-digital transducers (IDTs) from a harsh environment, which improves sensor stability. According to the best knowledge of the authors, there is no previous work in the literature comparing the conductometric sensitivity of surface acoustic modes in a layered structure.

The velocity change (Δv) of a surface wave due to a conductive thin film on the device surface calculated via perturbation theory is:²

$$\frac{\Delta v}{v} = \frac{-k^2}{2} \frac{1}{1 + \left(\frac{v_0 \epsilon_p}{\sigma_{sh}}\right)^2} \quad (1)$$

where k^2 is the electromechanical coupling coefficient, v_0 is the unperturbed propagation velocity, ϵ_p is the substrate permittivity and σ_{sh} is the sheet conductivity of the conductive layer. A normalised plot of Eq. (1) is shown in Figure 1. It can be seen that maximum velocity change, and hence maximum sensitivity, will occur when $\sigma_{sh} \approx v_0 \epsilon_p$.

By utilising an additional layer between the piezoelectric substrate and the gas selective layer, it is possible to

*Corresponding author; E-mail: david.powell@ieec.org

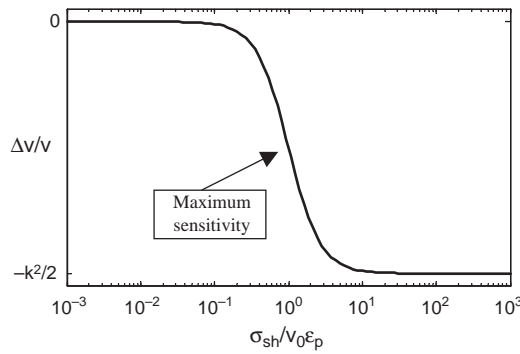


Fig. 1. Normalised conductivity sensitivity of a SAW device.

tailor the parameters, k^2 , v_0 and ϵ_p . The change in v_0 and ϵ_p allow the designer to match the product $v_0\epsilon_p$ of the substrate to σ_{sh} of the selective layer as shown in Figure 1, offering the possibility of increased sensitivity. However, when adding a dielectric layer, k^2 measured at the device surface (and hence sensitivity) will generally be reduced, since the surface is isolated from the piezoelectric substrate. By utilising a piezoelectric material such as ZnO, this effect is less prominent. For example, with a 1 μm SiO₂ layer and 24 μm wavelength, the electromechanical coupling of XZ LiNbO₃ is reduced to 1.06%, whereas for ZnO it is 2.96%, calculated by the method outlined in the subsequent section of this paper.

The addition of the layer to the SAW device can enhance or reduce the generation of different acoustic modes, and even create new modes. These modes will have different sensitivities to the conductivity change due to their differing values of k^2 , v_0 and ϵ_p . In the case of a layered SAW composed of isotropic materials, the parameter ϵ_p is expressed as:¹⁰

$$\epsilon_p = \epsilon_1 \frac{\epsilon_1 \tanh(\beta h) + \epsilon_2}{\epsilon_2 \tanh(\beta h) + \epsilon_1} + \epsilon_0 \quad (2)$$

where ϵ_1 and ϵ_2 are the dielectric constants of the layer and substrate respectively, h is the layer height, and β is the SAW propagation constant. For a non-layered SAW ($h = 0$), $\epsilon_p = \epsilon_2 + \epsilon_0$. The result is that the change in permittivity of the SAW structure due to the layer can be readily determined.

In the subsequent section it will be shown that the blank device allows propagation of only one Rayleigh mode. By depositing a ZnO layer, a shear horizontal (SH) mode is also generated which has particle displacement parallel to the surface and normal to the direction of propagation. The sensitivity of the two different modes propagating on a ZnO/XZ LiNbO₃ SAW sensor are determined and compared with theoretically obtained values of k^2 from a SAW effective permittivity analysis. The experimental gas sensing response is obtained by depositing an InO_x thin film onto the SAW device. InO_x is known to have a conductometric response to NO₂ gas.^{11,12}

2. THEORETICAL EVALUATION OF ACOUSTIC MODES

In order to investigate the presence of SAW modes in the considered structures, the effective permittivity has been calculated from the multi-layered SAW Green's function.^{13,14} The effective permittivity shows all acoustic modes, which can be piezoelectrically generated on a substrate, and can include the effect of layers. This function allows the quantities v_0 , k^2 and ϵ_p to be calculated. The singularities, where the function diverges, correspond to the SAW velocity with an electrical short circuit boundary condition, v_m . This velocity is dominant in determining the SAW centre frequency; hence it can be used to determine the centre frequency of any propagating modes. The zero crossing corresponds to the propagation velocity with an electrically open circuit boundary condition, v_f . The electromechanical coupling can be estimated¹⁵ from these velocities as

$$k^2 = 2 \frac{v_f - v_m}{v_f} \quad (3)$$

Effective permittivity is typically plotted as a function of $v^{-1} = \beta/\omega$, where β is the propagation constant, ω is angular frequency and v is the trial velocity. For comparison with measured frequency responses, β has been held constant at $2\pi/\lambda_0$, while ω is varied. The inter-digital transducer (IDT) period λ_0 is 24 μm . Figure 2 shows the calculated effective permittivity for XZ LiNbO₃, while Figure 3 is for 1 μm of (001) ZnO on an XZ LiNbO₃ substrate.

In Figure 2 a Rayleigh mode at 141.8 MHz is observed, with k^2 of 4.5% at the substrate-layer interface. After ZnO deposition (Fig. 3), the pole corresponding to the Rayleigh mode has been shifted to 138.2 MHz, with a k^2 of 5.9%. Another pole appears at 147.1 MHz, with a coupling of 0.18%. This is a SH propagation mode in the layered configuration, which is often referred to as a Love wave. Thus it can be seen that the addition of a layer above

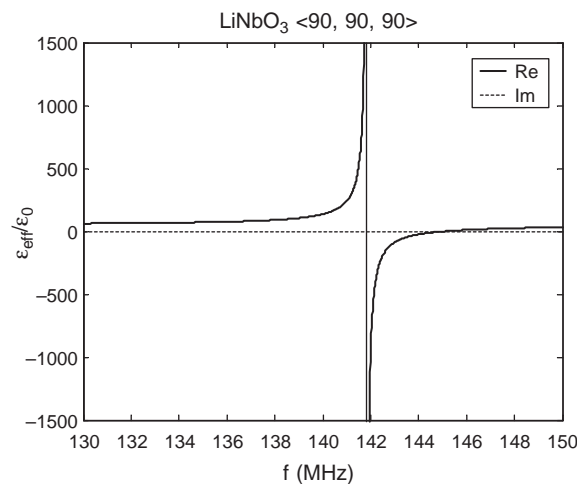


Fig. 2. The effective permittivity for the blank XZ LiNbO₃ device.

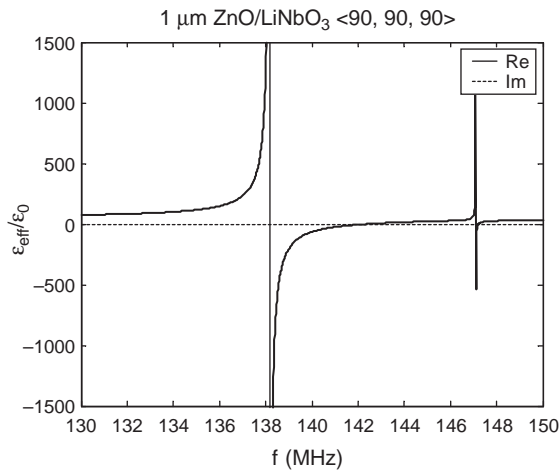


Fig. 3. Effective permittivity for the a 1 μm (001) ZnO film deposited onto XZ LiNbO₃.

the IDT increases the coupling between the IDT and the acoustic modes, as well as trapping a bulk shear mode to the surface.

The classification of each mode was performed by analysis of the particle displacement profiles. They are shown for the Rayleigh propagation mode on XZ LiNbO₃ in Figure 4 and for the Rayleigh and SH waves on ZnO/XZ LiNbO₃ in Figure 5 and Figure 6 respectively. As can be seen in Figure 4, the blank SAW device has strong sagittal displacement components u_x and u_z . After deposition of the ZnO layer the particle displacement is slightly perturbed but maintains its sagittal characteristic (Fig. 5). The additionally generated propagation mode has its predominant displacement component in the shear horizontal (u_y) direction.

In order to assess the conductometric sensitivity of the two modes, their electromechanical coupling at the surface needs to be calculated. This is conducted by calculating

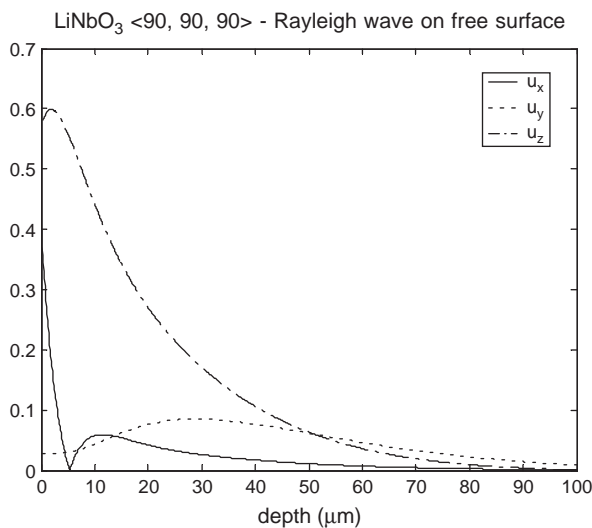


Fig. 4. Depth profile of Rayleigh wave at 142 MHz.

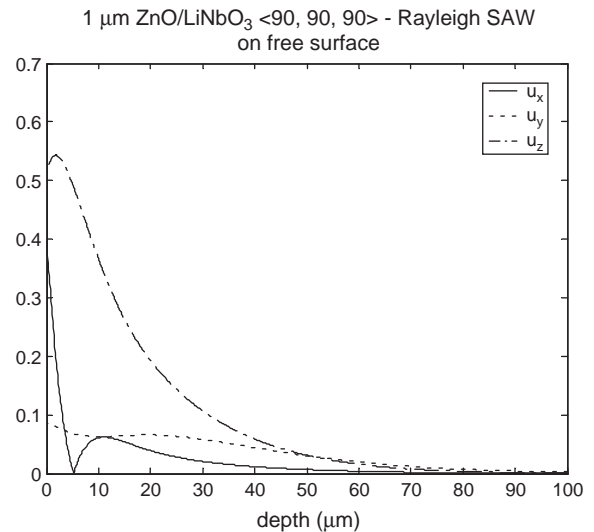


Fig. 5. Depth profile of Rayleigh wave at 138 MHz for the ZnO/LiNbO₃ structure.

the effective permittivity with the top of the device as the reference plane, and extracting the value of k^2 from this curve. For the Rayleigh mode it was found that the coupling was reduced to 2.96%. This can be explained by the fact that the voltage at the surface is being isolated from the substrate by the ZnO, which is a weaker piezoelectric than LiNbO₃. The SH mode was found to have a surface electromechanical coupling of 0.106%, which again is lower than the IDT coupling due to the isolating effect of the layer. As the conductometric sensitivity of a SAW device is proportional to its electromechanical coupling coefficient at the surface, it is expected that the sensitivity of the SH mode should be approximately 27 times less than the Rayleigh mode.

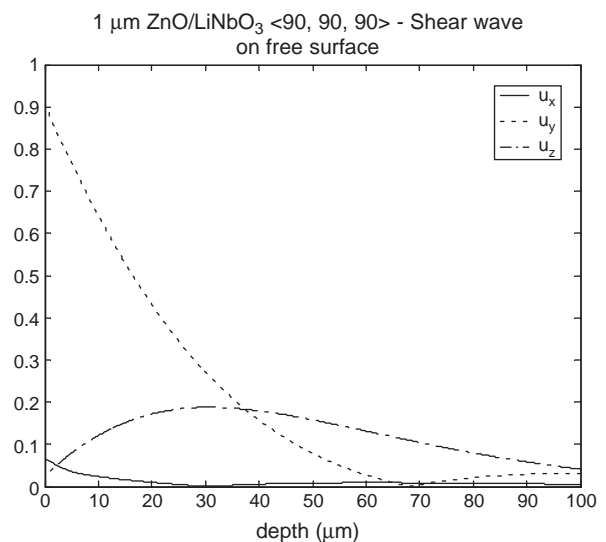


Fig. 6. Depth profile of shear wave at 147 MHz for the ZnO/LiNbO₃ structure.

3. EXPERIMENTAL SECTION

A SAW device has been fabricated on to a XZ LiNbO₃ substrate. It consists of 64 electrode pairs in input and output IDTs with periodicity of 24 μm . A 1 μm layer of ZnO was deposited by RF magnetron sputtering.

The 2 port S-parameters of the SAW device were measured using a network analyser, both before and after deposition of ZnO. Figure 7 shows the real part of the input admittance derived from the S-parameter measurements. This parameter was selected as it most clearly shows the excitation modes with greatly different k^2 . It can be seen that the large number of electrode pairs required to generate the SH mode results in excessive admittance for the Rayleigh mode, thus the Rayleigh mode is distorted by the triple transit effect. The frequencies corresponding to the metallised surface velocities have been marked for the Rayleigh and SH modes. It can be seen that in each case the centre of radiation conductance peak (ignoring distortion effects) lies just above this frequency, as expected.

A 20 nm layer of InO_x thin film has been deposited as the gas sensitive layer. This layer was deposited by RF magnetron sputtering of an indium target in a reactive oxygen atmosphere. Tests were conducted at an operating temperature of 150 °C. Response of the device towards NO₂ concentrations of 0.5 ppm, 1 ppm and 2 ppm were investigated for both operating modes.

An amplifier was incorporated in a closed loop with the SAW device to form an oscillator. The fractional shift in the frequency of the oscillator, upon the exposure to NO₂ gas, was the output signal. The sensor was locked in the Rayleigh and SH modes by a phase shift network incorporated into the closed loop. The resulting frequency shifts are plotted in Figure 8.

4. DISCUSSION

It can be seen that the dynamics of both responses are similar, but the magnitude of the Rayleigh mode response is approximately 19 times larger than the SH mode for

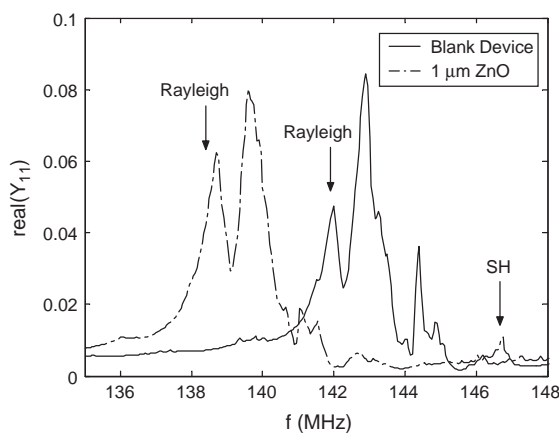


Fig. 7. Real part of input admittance before and after ZnO deposition.

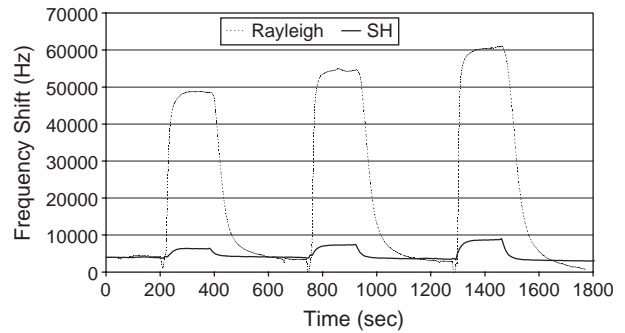


Fig. 8. Response to NO₂ gas: Comparison between the Rayleigh and SH modes.

0.5 ppm of NO₂. By inspection of Eq. (1), it can be seen that the sensitivities for the two modes should have the same ratio as their electromechanical coupling coefficients, which was calculated as 27.4.

It should be noted that for 1 ppm and 2 ppm the ratios of responses decrease to 14 and 11, respectively. Thus there is better agreement at low concentrations of NO₂. It was not possible to test lower concentrations with the existing test system. The authors believe that better agreement between calculations and measurements should be achieved for NO₂ concentrations lower than 0.5 ppm.

As these sensor responses are non-linear, it is proposed that a difference in saturation response of the two modes is occurring. Since the kinetics of the gas-sensor interaction are identical in both cases, the distinct conductivity sensitivities of the two modes should be responsible for the discrepancy. One possible explanation is the difference in the quantity $v_0 \epsilon_p$ between the modes, thus placing the operating region at different points in Figure 1.

It should also be noted that Eq. (1) was derived assuming that the piezoelectric interaction between the SAW and the conductive layer is weak.² For highly piezoelectric materials such as LiNbO₃, this assumption is incorrect. The equation also neglects the dependence of the wave characteristics on the electrical boundary conditions,¹⁶ particularly for non-Rayleigh wave modes, as well as the dispersion caused by the layer, which is dependant on the propagation mode. Thus a more accurate theory would be expected to show a slightly different curve to that in Figure 1, and would be dependant on the propagation mode. By using numerical techniques a more accurate conductivity-velocity relationship than that in Eq. (1) will be derived in the future.

5. CONCLUSION AND FUTURE WORK

The presence of different modes in layered SAW structures requires the selection of the most appropriate mode for sensing applications. Due to this fact, the study of the sensitivity of these modes is important. The presented work is believed to be an original theoretical and experimental

comparison of the conductometric sensitivity of multiple surface acoustic modes in layered structures.

Propagation properties of blank XZ LiNbO₃ and ZnO/XZ LiNbO₃ were theoretically compared using the multi-layered SAW Green's function. It was found that before ZnO thin film deposition the propagation mode is a Rayleigh type. After the thin film deposition an additional SH propagation mode is generated.

The ratio of experimental gas sensitivities was in good agreement with the ratio of the coupling coefficients, which were calculated using the Green's function method, for low NO₂ concentrations. For higher NO₂ concentrations the discrepancy between measured and calculated sensitivities increases. It is proposed to test the device towards NO₂ concentrations below 0.5 ppm to see if better agreement can be achieved. Additionally, further study is required to explain the discrepancy at higher gas concentrations.

References and Notes

1. H. Wohltjen and R. Dessy, *Anal. Chem.* 51, 1465 (1979).
2. A. J. Ricco, S. J. Martin, and T. E. Zipperian, *Sens. Actuators* 8, 319 (1984).
3. D'Amico, A. Palma, and E. Verona, *Sens. Actuators* 31 (1983).
4. S. J. Ippolito, S. Kandasamy, K. Kalantar-zadeh, A. Trinchi, and W. Wlodarski, *Sens. Lett.* 1, 33 (2003).
5. Y. R. Roh, Y. J. Lee, H. B. Kim, H. M. Cho, and S. Baik, *Sens. Actuators A: Phys.* 64, 173 (1998).
6. M. Penza and L. Vasanelli, *Sens. Actuators B: Chem.* 41, 31 (1997).
7. M. Penza, E. Milella, and V. I. Anisimkin, *Sens. Actuators B: Chem.* 47, 218 (1998).
8. J. Reibel, U. Stahl, T. Wessa, and M. Rapp, *Sens. Actuators B: Chem.* 65, 173 (2000).
9. K. Kalantar-zadeh, D. A. Powell, and W. Wlodarski, *Proc. 2004 IEEE Int. Ultrason. Symp.*, to be published.
10. K. Bløtekjær, K. A. Ingebrigtsen, and H. Skeie, *IEEE Trans. Elect. Dev.* 20, 1133 (1973).
11. R. Winter, K. Scharnagl, A. Fuchs, T. Doll, and I. Eisele, *Sens. Actuators B: Chem.* 66, 85 (2000).
12. G. Korotcenkov, I. Boris, V. Brinzari, B. Golovanov, Y. Lychkovsky, G. Kartotsky, A. Cornet, E. Rossinyol, J. Rodrigue, and A. Cirera, *Sens. Actuators B: Chem.* 103, 13 (2004).
13. D. A. Powell, K. Kalantar-zadeh, and W. Wlodarski, *Sens. Actuators A: Phys.* 115, 456 (2004).
14. Th. Pastureauud, V. Laude, and S. Ballandras, *Appl. Phys. Lett.* 80, 2544 (2002).
15. J. J. Campbell and W. R. Jones, *IEEE Trans. Son. Ultrason.* 15, 209 (1968).
16. L. Boyer, J. Desbois, Y. Zhang, and J. M. Hodé, *Proc. 1991 IEEE Ultrason. Symp.* 353 (1991).